Colloid Polym Sci (2009) 287:583–589
DOI 10.1007/s00396-009-2006-3

ORIGINAL CONTRIBUTION

# Effects of medium oil on electroresponsive characteristics of chitosan suspensions

**C. H. Hong · J. H. Sung · H. J. Choi**

Received: 14 December 2008 / Revised: 12 January 2009 / Accepted: 14 January 2009 / Published online: 7 February 2009


**Abstract** Biocompatible chitosan particle suspensions in host oils of corn, soybean, and silicone were prepared and their electrorheological (ER) characteristics were examined under the imposition of electric fields. The effects of the weight concentration of particulate chitosan and the strength of the applied electric field on ER response in the various chitosan particle suspensions were investigated via measurements of rheological properties including flow curve, shear viscosity, and yield stress. The yield stresses of the three different chitosan–oil systems showed different values of slope in the electric field, but all data were found to fit well with our previously proposed universal scaling function.

**Keywords** Electrorheological fluid · Chitosan · Electric field

## Introduction

Chitin, a biomacromolecule widely found in the shells of crabs, lobsters, shrimps, and insects, is one of the most abundant organic materials and second only to cellulose in terms of amount produced by biosynthesis. It consists of 2-acetamide-2-deoxy-β-D-glucose through the β-(1–4)-glycoside linkage. Though chitin fibers have been applied for making artificial skin and absorbable sutures [1], the insolubility of chitin in its native form in most organic solvents limits its engineering applications despite its abundance. However, biocompatible chitosan possessing free amino groups, poly[β-(1→4)-2-amino-2-deoxy-D-glucopyranose], the principal derivative of chitin with a partly deacetylated form produced by the alkaline deacetylation of chitin, is water-soluble and polycationic, possessing antimicrobial activities as well as the ability to absorb heavy metal ions. Because of these properties, chitosan has been widely used in applications in the fields of biochemistry, pharmacology, enzymology, microbiology, agriculture, and environmental studies as a natural biocompatible organic polymer. Because of its water-retaining and moisturizing properties [2], it has also been adopted in the cosmetics industry. Note that modified chitosans have been further prepared with various chemical and biological properties [3–5].

Meanwhile, chitosan particles dispersed in electrically non-conducting liquids have been reported as showing an electrorheological (ER) effect of rapid and reversible change in shear viscosity under an applied electric field [6,7]. In general, this ER phenomenon comes from the transient aggregation of the solid phase dispersed in the oil medium due to the attractive forces between the dipolar moments induced on each particle by the external field [8,9], along with their magnetically analogous magnetorheological suspensions under external magnetic fields [10,11]. The migration of mobile charges to areas with the greatest field concentration increases the polarizability of the particles and results in a larger dipole moment. These field-induced dipoles attract one another and cause the particles to form chains or fibrillated structures in the direction of the field. These chains are held together by interparticle forces that have sufficient strength to inhibit fluid flow.

The reversible nature of the ER response, the large change in shear viscosity and yield stress, and the short response times observed in these systems give rise to many useful technological applications. In addition, electrorheology can be achieved in a continuously variable, wide dynamic range that is energy efficient, fast, reliable, compact, and achievable at a reasonable cost. Therefore, ER fluid can be adopted in various mechanical devices such as shock absorbers, dampers [12,13], clutches, and engine mounts. Recently, biodegradable polymers have been tested for use as smart materials in work on the feasibility of using ER fluids as a controllable drug delivery system [14].

During the past four decades, early studies of the ER phenomenon covered many wet-based (hydrous) suspen-

C. H. Hong · J. H. Sung · H. J. Choi (✉)
Department of Polymer Science and Engineering, Inha University, Incheon 402-751, South Korea
e-mail: hjchoi@inha.ac.kr

sions [15]. However, to overcome the shortcomings such as instability and corrosion that wet-based systems possess, various dry-based (anhydrous) systems with anhydrous particles, zeolite [16] and intrinsically polarizable semiconducting polymers, have been investigated. ER fluids are in general non-aqueous suspensions composed of electrically polarizable particles dispersed in a dielectric fluid, and the disperse phases play a very important role in the ER phenomenon. Anhydrous ER materials are polarizable with conducting and electroluminescent material, including polyaniline and its derivative [17–20], PMMA particles with a polyaniline coating [21], polypyrrole [22], poly (acene quinone) radicals [23], and poly(*p*-phenylene) [24]. Synthetic organic polymers of polyphenol and polyurethane possessing branched polar groups such as amino (—$NH_2$), hydroxy (—OH), and amino-cyan (—NHCN) have also been used as disperse phases of ER fluids. Furthermore, cellulose and starch as natural organic polymers have also been adopted as disperse phases for ER materials.

These polar groups may affect the ER behavior by playing the role of the electronic donor, so that the chemical structure of the organic materials is regarded to be an important factor in the ER effect [25]. Recently, chitosan and chitosan derivatives such as chitosan phosphate [6], chitosan sulfate, and dihydroxylpropyl chitosan [26] have been introduced as new anhydrous disperse phases in ER fluid systems.

In this study, we adopted chitosan particles as anhydrous particles in dry-based ER fluids. ER systems based on chitosan particles in soybean, corn, and silicone oils were examined for electrical and rheological properties, including yield stress of the ER fluids, in order to understand how different oils affect ER performance.

## Experimental methods

Chitosan, a natural organic polymer derived from chitin by *N*-deacetylation and composed of poly-D-glucosamine, is a series of different deacetylated (higher than 50%) chitin derivatives and the only amino polysaccharide which is widely distributed in huge amounts in nature. Chitosan, on the other hand, is a cationic polyelectrolyte because the amino group in the backbone of the molecule is protonated in acidic solutions. The chemical reaction diagram of chitosan is as follows:

The chitosan used as anhydrous ER material was a commercial powder with a deacetylation degree of about 95% and supplied by Samchully Pharm. (Korea). Chitosan was put into a vacuum oven for approximately 2 days for drying to remove any trace of moisture. ER fluids were then prepared by dispersing the chitosan particles in three different oils, e. g., corn oil, soybean oil, and silicone oil, which were dried in a vacuum oven and stored with 100-μm molecular sieves prior to use. Desired amounts of chitosan particles for four different particle concentrations of 10, 15, 20, and 25 wt.% were put into the 50-ml bottles with soybean oil and then mechanically uniformly dispersed using both an automatic shaker and an ultrasonicator. The same method was applied for both corn oil and silicone oil for 25 wt.% chitosan particle. The densities of the corn oil and soybean oil were about 0.92 g/ml and that of the silicone oil was 0.96 g/ml at 25°C. In addition, the viscosity of these oils was 50 cS.

The electrical conductivity of the chitosan particles was measured to be $5.26 \times 10^{-10}$ S/cm. For the conductivity measurement of the chitosan particles using a two-probe method, pellets of dried chitosan particles were prepared using a 13-mm KBr pellet die, and then the resistance of the pellets was measured using a picoammeter (Keithley model 487, Cleveland, OH, USA) with a conductivity cell. The conductivity ($\sigma$) was then calculated from the relationship $\sigma = d/(R \cdot A)$ using the surface area ($A$), the thickness ($d$), and the resistance ($R$) of the pellet. The electrorheological properties of the chitosan-based ER fluids were measured using a rotational rheometer (Physica MC120, Stuttgart, Germany) with a Couette geometry (Z3-DIN) equipped with a high-voltage generator (HVG 5000, Stuttgart, Germany). Temperature was controlled through a circulating oil bath (Viscotherm VT 100). Several DC electric field strengths (0.5–3.0 kV/mm) were applied to the insulated bob. The flow curve was then measured from the controlled shear rate (CSR) mode as a shear rate was applied to the ER fluid and the resulting shear stress was measured. In the controlled shear stress (CSS) mode, the ER fluid was stressed by an applied mechanical torque until the particle chain was broken to generate flow, and the stress at the onset of flow was reported as a static yield stress. Note that the yield stress is greatly affected by the electric field strength and increases with particle concentration [7].

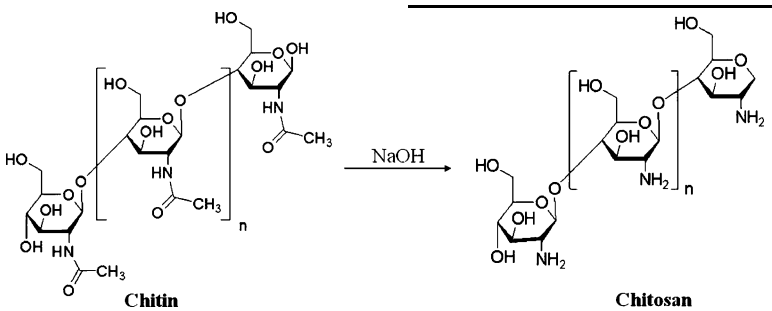

## Results and discussion

Figure 1 shows an SEM photograph of chitosan particles, showing particle size distribution, irregular particle shape, and particle sizes in the range of 50–300 μm. The Fourier transform infrared spectroscopy (FT-IR) spectrum of the chitosan determined using KBr pellets is given in Fig. 2. The peak at 3,000~4,000 $cm^{-1}$ originates from the OH and $NH_2$, whereas the peaks at 1,716 $cm^{-1}$ is due to C═O of $NHCOCH_3$, and those at 2,900 $cm^{-1}$ and 1,350 $cm^{-1}$ are the C—H stretching and C—H bending modes. In addition, chitosan particles have a good thermal stability.

As for the thermal properties of chitosan, its thermogravimetric analysis (TGA) result in a nitrogen atmosphere at a heating rate of 20°C/min is represented in Fig. 3. The thermal degradation characteristics of chitosan in nitrogen gas surroundings showed three distinct regions. At the first step, thermal degradation of the chitosan begins from 105°C to 265°C with its weight loss of about 11 wt.%. The second step of degradation is the fastest degradation from 265°C to 330°C with its loss of about 45 wt.%. The final step of degradation is widely ranged from 330°C to 765°C, resulting in its complete thermal degradation.

Figure 4a, b shows flow curves measured from the CSR mode using a rotational rheometer with a Couette geometry for the 25-wt.% chitosan-based ER fluids dispersed in corn oil at various electric field strengths. The solid line in Fig. 4a is fitted using the following CCJ model [27]:

$$\tau = \frac{\tau_{yd}}{1 + (t_1 \dot{\gamma})^{\alpha}} + \eta_{\infty}\left(1 + \frac{1}{(t_2 \dot{\gamma})^{\beta}}\right)\dot{\gamma} \qquad (1)$$

Here, $\alpha$ is related to the decrease in shear stress while $\beta$ is weakly related to the term of shear stress increase in a high shear rate region; $t_1$ and $t_2$ are time constants and $\eta_{\infty}$ is the shear viscosity at a high shear rate in the absence of an electric field. The above six-parameter model can describe the stress decrease phenomena in a low shear rate region as well as provide an accurate estimate for the dynamic yield stress ($\tau_{yd}$) when we fit the experimental data. The first term in Eq. 1 describes the decrease of shear stress with increase in shear rate at a low shear rate region and the second term is responsible primarily for the contribution of the shear stress at a high shear rate region. Note that shear stress depends directly either on the particle interactions or on the derivative of the electrostatic energy with respect to the shear strain. The optimal parameters to fit the data using this model are summarized in Table 1. The coefficient $\alpha$ depends on the particle concentration. The $\beta$ values are 0.1452, 0.0609, 0.6005, 0.4671, and 0.4463 for various electric fields with 0.5, 1.0, 1.5, 2.0, and 3.0 kV/mm, respectively.

Figure 4a shows that, in the absence of an electric field, the fluid behavior is similar to that of a Newtonian fluid.

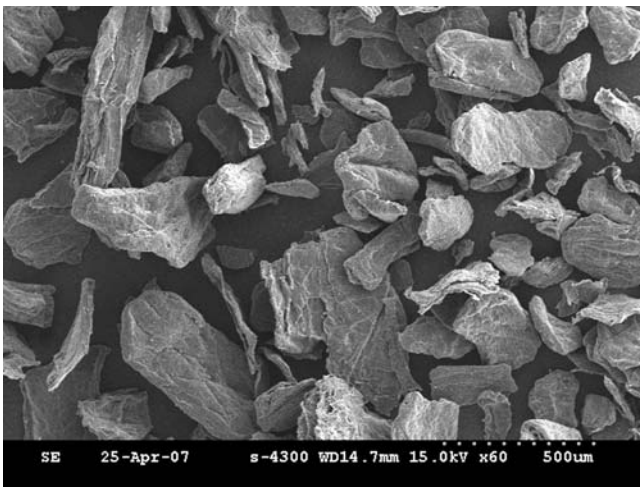


**Fig. 1** SEM photograph of chitosan

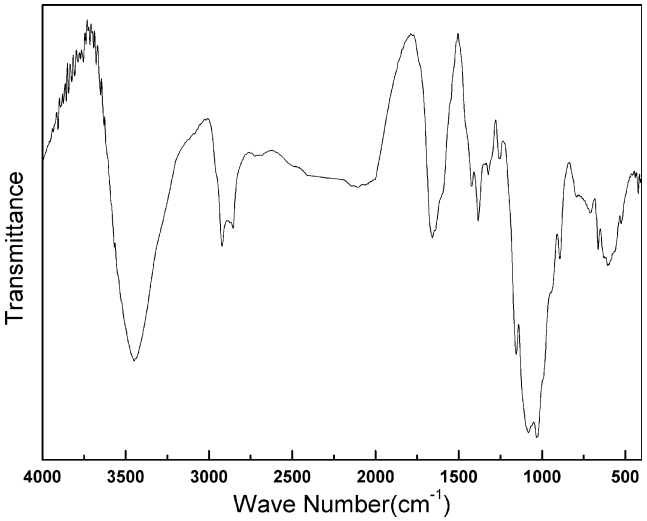


**Fig. 2** FT-IR spectra of chitosan

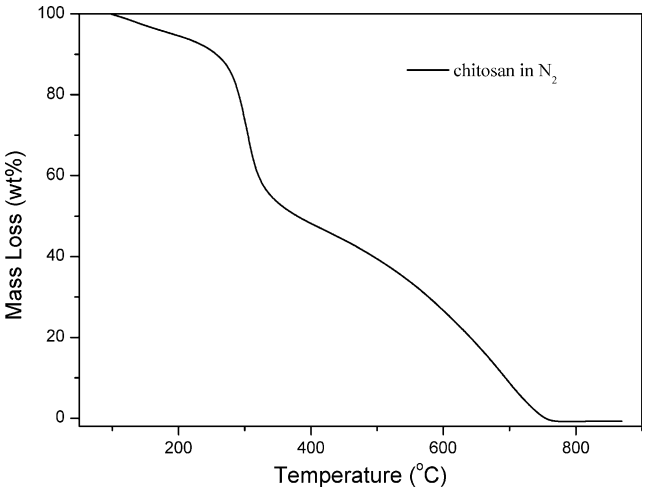


**Fig. 3** TGA of chitosan

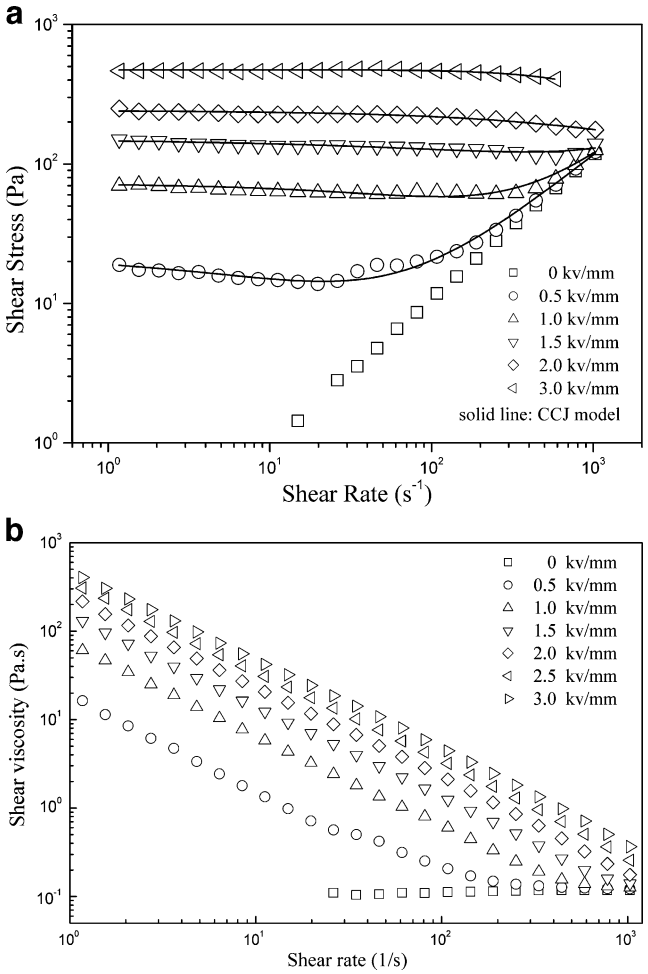


**Fig. 4** **a** Shear stress vs. shear rate of chitosan–corn oil suspension (25 wt.%) for various electric field strengths at 25°C. **b** Shear viscosity vs. shear rate of chitosan–corn oil suspension (25 wt.%) under various electric field strengths at 25°C

When an electric field is applied to the suspension, shear stresses measured with increasing the shear rate increased with the electric field strength, mainly due to an interparticle interaction force. The shear stress remained almost constant, exhibiting a plateau region over a quite wide range of shear rate as the shear rate increased up to a certain value, e. g., 100 $s^{-1}$ for 0.5 kV/mm, 400 $s^{-1}$ for 1.0 kV/mm, and 800 $s^{-1}$ for 1.5 kV/mm, increasing with the electric field strength, indicating that the electrostatic force becomes dominant over the hydrodynamic force. On the other hand, shear stress appears to converge to the zero-electric field strength value above the transition shear rate, as can be clearly seen in Figure 4a in the cases of 0.5, 1.0, and 1.5 kV/mm.

Figure 4b represents the apparent viscosity of the same ER fluid measured in Fig. 4a at different electric fields, in which the shear viscosity curve shows a shear-thinning phenomenon. The shear viscosity increment under an applied electric field at low shear rate is related to the increased hydrodynamic volume of the system, resulting in increased viscous dissipation. When a shear strain with increased shear rate is applied to the aligned structures, it distorts and destroys the fibril chains and finally demonstrates the decrease of the shear viscosity of a shear-thinning behavior.

Figure 5a, b shows flow curves measured from the CSR mode for the ER fluid systems of chitosan dispersed in soybean oil at 2 kV/mm for four different particle concentrations of 10, 15, 20, and 25 wt.%. Shear stresses increase with increasing particle concentration over the entire shear rate range. The concentrated ER fluid is considered to possess thicker particle chain fibril than the less concentrated ER fluid. Nonetheless, the sudden increase of shear stress for 15 wt.% is noteworthy. Particle concentration effect on shear stress for various ER fluids has been observed to be nonlinear as a function of particle concentration [28,29]. This might be related to percolation threshold not only for the ER fluids but also for general particle suspension. However, in the case of ER fluid, its effect could be dominant due to the formation of thick columns. Detailed and careful investigation on particle effect for the ER fluids requires further study. In general, the structure in a concentrated suspension is sufficiently rigid to enable the material to withstand a certain level of deforming stress without flowing to occur. These flow curves show similar trends in both the corn and silicone oil systems.

Figure 6 illustrates the effect of the concentration of chitosan particles in silicone oil on static yield stress for various applied electric field strengths using the CSS mode.

**Table 1** The optimal parameters in CCJ model equation obtained from the flow curve of chitosan–corn oil suspension ER fluids at various electric field strengths

| Model | Parameters | 0.5 kV/mm | 1.0 kV/mm | 1.5 kV/mm | 2.0 kV/mm | 3.0 kV/mm |
|---|---|---|---|---|---|---|
| CCJ | $\tau_{yd}$ | 23 | 72 | 150 | 241 | 470 |
| | $t_1$ | 0.0513 | 0.0038 | 0.0003 | 0.0002 | 0.0005 |
| | $\alpha$ | 0.5408 | 0.6789 | 0.4430 | 0.5689 | 1.2561 |
| | $\eta_\infty$ | 0.0552 | 0.0496 | 0.0338 | 0.0041 | 0.0033 |
| | $t_2$ | 0.00065 | 0.00121 | 0.04707 | 0.00999 | 0.00001 |
| | $\beta$ | 0.1452 | 0.0609 | 0.6005 | 0.4671 | 0.4463 |

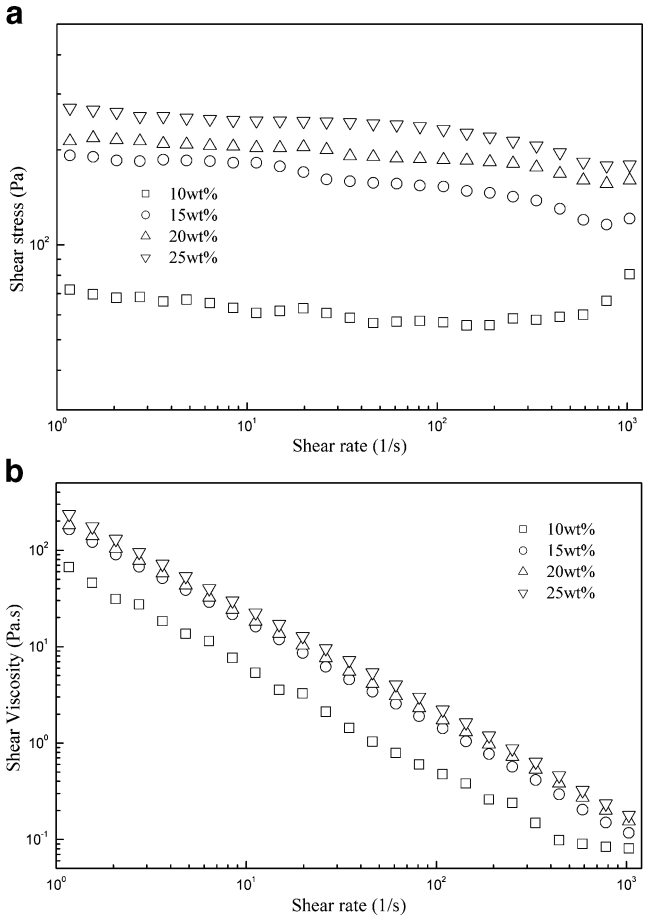


**Fig. 5** **a** Shear stress vs. shear rate for chitosan in soybean oil at four different particle concentrations and electric field strength of 2 kV/mm. **b** Shear viscosity vs. shear rate of chitosan in soybean oil at four different electric field strengths at 25°C

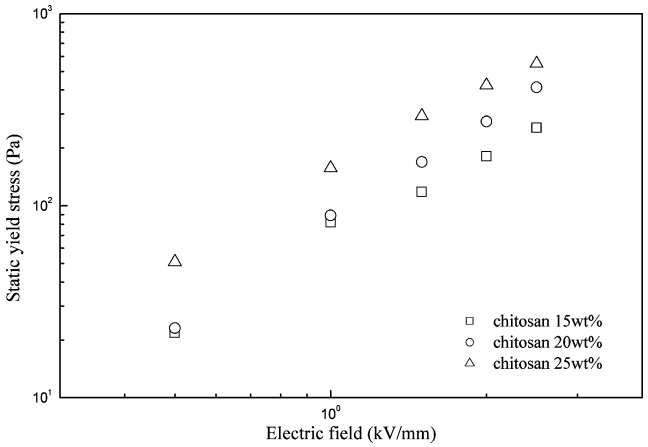


**Fig. 6** Static yield stress of the concentration of chitosan particles in silicone oil under various electric field strengths

The increase of the static yield stress as a function of the concentration of chitosan through increasing the imposed electric field strength is noteworthy.

Flow curves and shear viscosity of the chitosan ER fluids for the 25 wt.% chitosan particle with different oil systems at 2.0 kV/mm are shown in Fig. 7, subpanels a and b, respectively. The magnitude of shear stress of the chitosan–silicone system is observed to be slightly higher than that of the chitosan and corn or soybean oil systems. In the case of the silicone system, the interaction between the chitosan particles and the host oil has been interpreted based on dielectric spectra and polarizability [30].

Figure 8 presents the dependence of static yield stress ($\tau_y$) on electric field strength for chitosan-based ER fluids (25 wt.%) with three different oils obtained from the CSS mode. Generally, the correlation of the static yield stress

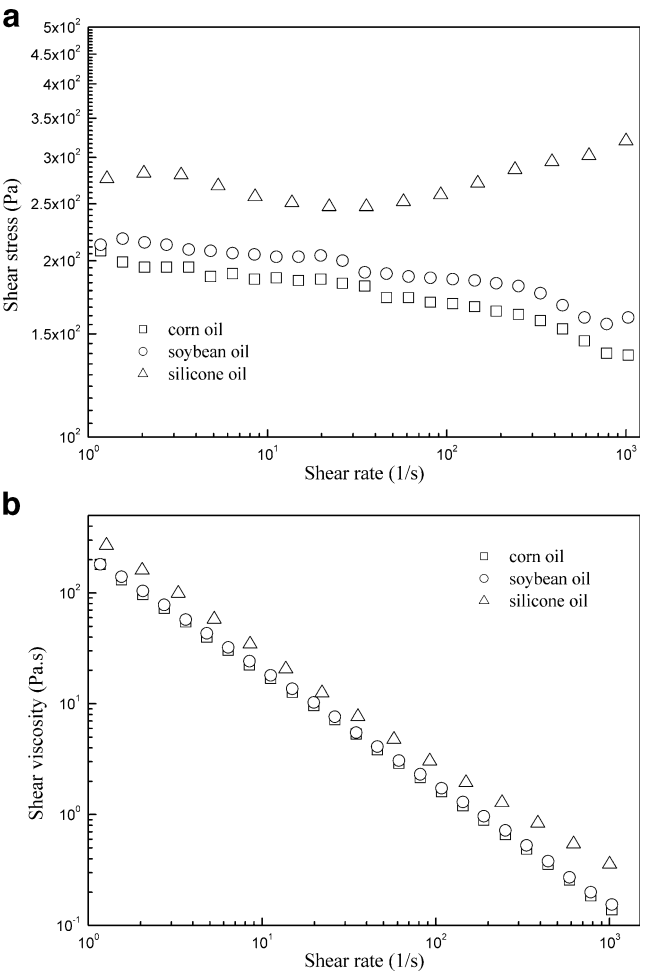


**Fig. 7** **a** Shear stress vs. shear rate for chitosan (25 wt.%) in three oil systems under the electric field strength of 2 kV/mm at 25°C. **b** Shear viscosity vs. shear rate for chitosan (25 wt.%) in three oil systems under the electric field strength of 2 kV/mm at 25°C

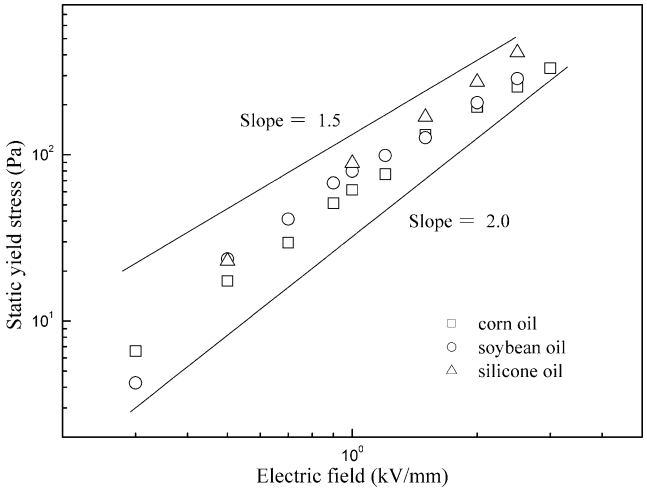


**Fig. 8** Static yield stress vs. electric field strength for chitosan (25 wt.%) in three different oils at 25°C

($\tau_y$) to the electric field strength ($E$) is presented as follows [31,32]:

$$\tau_y \propto E^x \tag{2}$$

The $x$ values in this study were observed for various oils: corn oil—1.72, soybean oil—1.86, and silicone oil—1.78, and these numbers differ slightly from the predicted values based on the polarization model [32,33], in which the yield stress is proportional to the electric field strength $E^2$. The polarization model with the point-dipole approximation is a rather ideal system compared to our real chitosan-based ER systems. The shape of our chitosan particles was very irregular, as can be observed from the SEM in Fig. 1. The yield stress of ER fluids is known to be greatly affected by both electric field strength and particle concentration. Figure 8 represents a correlation between yield stress and electric field strength. To correlate yield stress with electric field strengths in the broad range, Choi et al. [34] introduced the following universal yield stress equation which incorporates both the polarization and conduction models.

$$\tau_y(E_0) = \kappa E_0^2 \left( \frac{\tanh \sqrt{E_0/E_c}}{\sqrt{E_0/E_c}} \right) \tag{3}$$

where $\kappa$ depends on the dielectric constant and the particle volume fraction and $E_c$ is the critical electric field strength, which is proportional to the particle conductivity. Various ER materials including poly(*p*-phenylene) [35], mesoporous MCM-41 [36], and polypyrrole/MCM-41 composite [37] have been reported to follow Eq. 3

Equation 3 has the following two limiting behaviors at low and high electric field strengths:

$$\tau_y(E_0) = \kappa E_0^2 \text{ for } E_0 \ll E_c \tag{4}$$

and

$$\tau_y(E_0) = \kappa \sqrt{E_c} E_0^{3/2} \text{ for } E_0 \gg E_c \tag{5}$$

Equation 4 indicates that $\tau_y$ is proportional to $E_0^2$ at low $E_0$, as expected from the polarization model. Equation 5 indicates that $\tau_y$ is proportional to $E_0^{3/2}$ at high $E_0$, as predicted from the conductivity model.

In order to examine the correlation of the data with the universal curve using the normalized scaling function [34], the following equation was used:

$$\hat{\tau} = 1.313 \hat{E}^{3/2} \tanh \sqrt{\hat{E}} \tag{6}$$

where $\hat{E} \equiv E_0/E_c$ and $\hat{\tau} \equiv \tau_y(E_0)/\tau_y(E_c)$. As it has been fully explained in our previous work [18], the beauty of these correlations is the fact that most of the ER experimental data can be collapsed with a parameter $E_c$ which is qualitatively related to particle properties and conductivity mismatch between particle and medium. The chitosan data are collapsed onto a single curve using Eq. 6, which is shown in Fig. 9. $E_c$ values for chitosan–oil systems are estimated to be 1 kV/mm in corn oil, 1.2 kV/mm in soybean oil, and 0.3 kV/mm in silicone oil, respectively, and it is interesting to note that $E_c$ for these different oils at the same particle concentration are different possibly due to conductivity or dielectric constant mismatch between particle and medium. The detailed procedure to get the universal yield stress plot of Fig. 9 is the same as in our previous work [18].

## Conclusion

Chitosan suspensions in three different oils showed ER response upon the application of an electric field. The shear stress and shear viscosity increased with both electric field

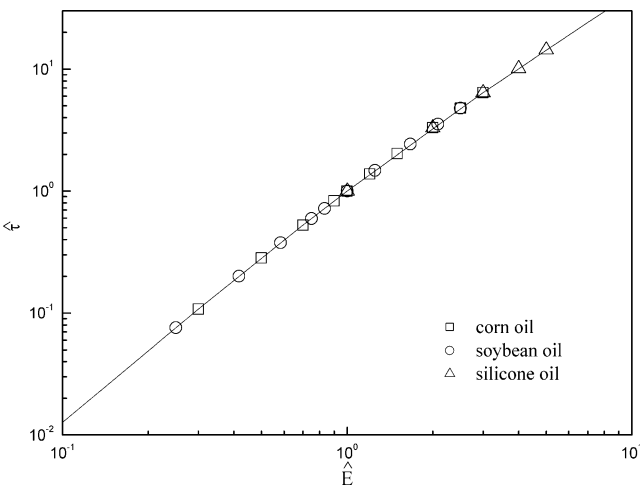


**Fig. 9** The universal curve for $\hat{\tau}$? vs. $\hat{E}$? for chitosan (25 wt.%) in three different oils

strength and particle concentration for all oil mediums. The yield stress of chitosan dispersed in silicone oil was higher than that of the other oil suspensions and correlated very well with the universal scaling curve.

**Acknowledgement** This study was supported by Fundamental R&D Program for Core Technology of Materials, Ministry of Knowledge Economy (2008).

## References

1. Kurita K (1998) Polym Degrad Stab 59:117–120
2. Muzzarelli RAA (1986) Chitin in nature and technology. Plenum, New York
3. Shahidi F, Arachchi JKV, Jeon YT (1999) Trends Food Sci Tech 10:37–51
4. Lee KY (2007) Macromol Research 15:195–201
5. Cho J, Heuzey MC, Begin A, Carreau PJ (2005) Biomacromolecules 6:3267–3275
6. Choi US, Ko YG, Kim TY (2000) Polym J 32:501–504
7. Sung JH, Choi HJ, Jhon MS (2002) Mater Chem Phys 77:778–783
8. Fang FF, Choi HJ, Joo J (2008) J Nanosci Nanotech 8:1559–1581
9. Trlica J, Sáha P, Quadrat O, Stejskal (2000) J Physica A 283:337–348
10. Bica I, Choi HJ (2008) Int J Mod Phys B 22:5041–5064
11. Bica I (2007) J Ind Eng Chem 13:299–304
12. Kim JW, Choi HJ, Lee HG, Choi SB (2001) J Ind Eng Chem 7:218–222
13. Choi SB, Han SS, Sung KG, Lee YS, Han MS (2006) Smart Mater Struc 15:850–858
14. Davies JL, Blagbrough IS, Staniforth JN (1998) Chem Commun 19:2157–2158
15. See H (1999) Korea-Aust Rheol J 11:169–195
16. Cho MS, Choi HJ, Chin J, Ahn WS (1999) Micropor Mesopor Mater 32:233–239
17. Lu J, Zhao XP (2002) J Mater Chem 12:2603–2605
18. Kim SG, Lim JY, Sung JH, Choi HJ, Seo Y (2007) Polymer 48:6622–6631
19. Choi HJ, Cho MS, To K (1998) Physica A 254:272–279
20. Trlica J, Sáha P, Quadrat O, Stejskal J (1999) J Phys D: Appl Phys 33:1773
21. Choi HJ, Hong CH, Jhon MS (2007) Int J Mod Phys B 21:4974–4980
22. Kim DH, Kim YD (2007) J Ind Eng Chem 13:879–894
23. Choi HJ, Cho MS, Jhon MS (1999) Int J Modern Phys B 13:1901–1907
24. Vaschetto ME, Monkman AP, Springborg M (1999) J Mol Structure Theochem 468:181–191
25. Choi HJ, Jhon MS (2009) Soft Matter. doi:10.1039/<b818368f>
26. Wu SZ, Zeng F, Shen JR (1998) J Appl Polym Sci 67:2077–2082
27. Cho MS, Choi HJ, Jhon MS (2005) Polymer 46:11484–11488
28. Kim SG, Kim JW, Choi HJ, Suh MS, Shin MJ, Jhon MS (2000) Colloid Polym Sci 278:894–898
29. Sung JH, Park DP, Park BJ, Choi HJ, Jhon MS (2005) Biomacromolecules 6:2182–2188
30. Sung JH, Jang WH, Choi HJ, Jhon MS (2005) Polymer 46:12359–12365
31. Block H, Kelly JP (1988) J Phys D: Appl Phys 21:1661–1677
32. Klingenberg DJ, Swol FV, Zukoski CF (1991) J Chem Phys 94:6170–6178
33. Yoon DJ, Kim YD (2007) J Mater Sci 42:5534–5538
34. Choi HJ, Cho MS, Kim JW, Kim CA, Jhon MS (2001) Appl Phys Lett 78:3806–3808
35. Sim IS, Kim JW, Choi HJ, Kim CA, Jhon MS (2001) Chem Mater 13:1243–1247
36. Cho MS, Choi HJ, Ahn WS, Jhon MS (2002) Stud Surf Sci Catal 141:479–486
37. Cheng Q, Pavlinek V, Lengalova A, Li C, Belza T, Saha P (2006) Micropor Mesopor Mater 94:193–199